*J. Fluid Mech.* (2015), *vol.* 784, R3, doi:10.1017/jfm.2015.618

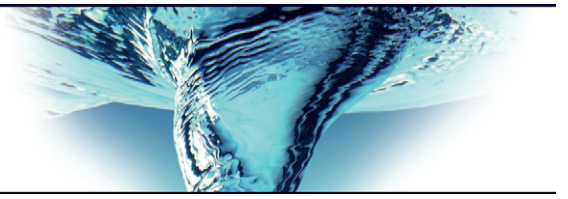

JFM RAPIDS
journals.cambridge.org/rapids

# Effects of polymer additives in the bulk of turbulent thermal convection

**Yi-Chao Xie[1], Shi-Di Huang[1], Denis Funfschilling[2], Xiao-Ming Li[1], Rui Ni[1,‡] and Ke-Qing Xia[1,†]**

[1]Department of Physics, The Chinese University of Hong Kong, Shatin, Hong Kong, China

[2]LRGP, Lorraine University, CNRS, 1 rue Grandville B.P. 20451, F-54001 Nancy, France

(Received 11 September 2015; revised 15 October 2015; accepted 19 October 2015; first published online 4 November 2015)

We present experimental evidence that a minute amount of polymer additives can significantly enhance heat transport in the bulk region of turbulent thermal convection. The effects of polymer additives are found to be the enhancement of coherent heat fluxes and suppression of incoherent heat fluxes. The enhanced heat transport is associated with the increased coherency of thermal plumes, as a result of the suppression of small-scale turbulent fluctuations by polymers. The incoherent heat flux, arising from turbulent background fluctuations, makes no net contribution to heat transport. The fact that polymer additives can increase the coherency of thermal plumes is supported by the measurements of a number of local quantities, such as the extracted plume amplitude and width, the velocity autocorrelation functions and the velocity–temperature cross-correlation coefficient. The results from local measurements also suggest the existence of a threshold value for the polymer concentration, only above which significant modification of the plume coherent properties and enhancement of the local heat flux can be observed. Estimation of the plume emission rate suggests a stabilization of the thermal boundary layer by polymer additives.

**Key words:** Bénard convection, plumes/thermals, polymers

## 1. Introduction

The ability to efficiently transport heat, momentum and mass is one of the hallmarks of turbulent flows, which finds numerous examples in both industry and daily life. One way to enhance mass transport, or equivalently to reduce wall drag, is to seed the turbulent flow with tiny amount of long-chain polymers (Toms 1948). The

† Email address for correspondence: kxia@phy.cuhk.edu.hk

‡ Present address: Department of Mechanical and Nuclear Engineering, Pennsylvania State University, State College, PA 16802-1412, USA.

so-called polymer-induced drag reduction has been studied extensively (see, for example, Procaccia, L'vov & Benzi 2008). Compared with drag reduction, the effects of polymer additives on turbulent heat transport, via turbulent thermal convection, for instance, have just started to draw attention very recently (Ahlers & Nikolaenko 2010; Benzi, Ching & De Angelis 2010; Boffetta *et al.* 2010; Wei, Ni & Xia 2012; Benzi, Ching & Chu 2012).

An idealized model to investigate turbulent thermal convection is turbulent Rayleigh–Bénard convection (RBC), which is a closed system of a fluid layer confined between two horizontally parallel plates heated from below and cooled from above (Ahlers, Grossmann & Lohse 2009; Lohse & Xia 2010; Chillá & Schumacher 2012; Xia 2013). This system is controlled by two dimensionless parameters, i.e. the Rayleigh number $Ra = \alpha g \Delta T H^3/(\nu\kappa)$ and the Prandtl number $Pr = \nu/\kappa$, where $g$ is the gravitational acceleration constant, $\Delta T$ is the temperature difference across the plates separated by a distance $H$, and $\alpha$, $\nu$ and $\kappa$ are respectively the thermal expansion coefficient, the kinematic viscosity and the thermal diffusivity of the fluid. The salient feature of turbulent RBC is the existence of distinct flow regions, i.e. the laminar, albeit fluctuating, thermal boundary layers (BLs) in the vicinity of the top and bottom walls (Sun, Cheung & Xia 2008; Zhou & Xia 2010; Zhou *et al.* 2010) and a turbulent bulk region far away from the walls. The flow in the bulk region has been shown to be close to homogeneous turbulent thermal convection (Lohse & Toschi 2003; Calzavarini *et al.* 2005).

With the presence of polymers, one thus needs to consider these two regions separately due to their different flow dynamics. It has been shown in turbulent bulk flows in which temperature is not a dynamic variable that the energy cascade process is strongly modified by polymer additives (Crawford *et al.* 2008; Ouellette, Xu & Bodenschatz 2009; Xi, Bodenschatz & Xu 2013). In the bulk flow of turbulent RBC, where there are strong temperature and velocity fluctuations, it is proposed that polymer additives can enhance the heat transport (Benzi *et al.* 2010). In contrast, it is suggested that polymer additives stabilize the thermal BL, which reduces the emission of thermal plumes and hence the heat transport (Ahlers & Nikolaenko 2010; Wei *et al.* 2012). The global Nusselt number $Nu$ (the total heat flux normalized by the one that would prevail by conduction alone) is then determined by the competition of these two effects. Although the aforementioned ideas could provide a plausible explanation of the observed heat transport enhancement in homogeneous turbulent thermal convection and heat transport reduction in the boundary-layer-dissipation-dominated regime of turbulent RBC, direct evidence based on local measurements is still missing, which motivates the present study of the effects of polymer additives in the bulk of turbulent RBC.

## 2. The experiments

The experiments were carried out in a cylindrical convection cell with a diameter $D$ (height $H$) of 19.3 cm (19.5 cm). Deionized and degassed water was used as the working fluid. The detailed design of the convection cell has been reported elsewhere (Qiu, Xia & Tong 2005; Wei *et al.* 2012). Here, we mention only the essential features. The convection cell was an upright plexiglass cylinder with aluminium rough top and bottom plates whose surfaces were coated with a thin layer of Teflon. The roughness was in the form of pyramids with a height of 8 mm that were arranged in a square lattice, and was machined directly on the plates. The vertex angle of the roughness was 90°. It is suggested that in the present parameter range of $Ra$ and $Pr$,

both energy and thermal dissipations are bulk-dominated in convection cells with rough surfaces compared with those in the cases with smooth surfaces (Wei *et al.* 2014), which motivated us to carry out experiments in the rough cell.

The convective heat flux, i.e. local Nusselt number, at the cell centre was measured using a small thermistor (Measurement Specialties, G22K7MCD419) combined with a two-dimensional laser Doppler velocimeter (LDV, Dantec Dynamics), which were similar to those used in Shang *et al.* (2003, 2004). The thermistor used had a time constant of 30 ms in water and a diameter of 0.3 mm. The spatial separation between the LDV focusing point and the thermistor tip was ∼0.8 mm, which was much smaller than the correlation length between temperature and velocity fluctuations (Shang *et al.* 2004). The temperature and velocity measurements were synchronized in such a way that when a velocity burst was captured by the LDV processor, it would record the temperature simultaneously. Using the acquired temperature $T(t)$ and velocity $u(t)$ with an averaged sampling rate of ∼60 Hz, we obtained the instantaneous normalized local convective heat flux,

$$J_\alpha(t) = (u_\alpha(t) \times \delta T(t))\ H/(\kappa \Delta T), \tag{2.1}$$

where $\alpha = z$ and $x$ are for the vertical and horizontal directions respectively; $\delta T(t) = T(t) - T_0$ is the temperature deviation from the mean temperature $T_0$ measured at the cell centre. In addition, the temperature signal itself was separately recorded by a digital-to-analogue converter at a sampling rate of 64 Hz, and the data were used in the analysis of plume dynamics. All measurements were conducted at a fixed input power at the bottom plate (or constant heat flux, 484 W), while maintaining the bulk temperature of the fluid at 40 °C. The corresponding Rayleigh and Prandtl numbers were $Ra = 6.18 \times 10^9$ and $Pr = 4.3$ for the Newtonian case. To obtain sufficient statistics, each measurement lasted for 12 h, corresponding to ∼1400 turnover times of the largest eddy in the system.

Polyacrylimide (PAM; Polysciences 18522-100) with nominal molecular weight $Mw = 18 \times 10^6$ atomic mass units (amu) was used in the experiment. The polymer concentration $c$ was varied from 0 to 24 parts per million (ppm) by weight. The effects of polymer additives on the thermodynamic properties of water at such dilute concentrations are negligible except for the fluid viscosity (Rubinstein & Colby 2003). The measured fluid viscosity was increased by up to 30 % from the pure water value in the present study.

The Weissenberg number $Wi = \tau_p/\tau_\eta \sim 0.1$ for PAM, where $\tau_p$ is the polymer relaxation time based on the Zimm model (Zimm 1956) and $\tau_\eta$ is the Kolmogorov time scale directly measured using particle tracking velocimetry at the cell centre. We remark that the value of $Wi$ estimated above is a spatially and temporally averaged quantity. It is known that strong temperature and velocity fluctuations occur in turbulent RBC. Thus, instantaneous stretching of polymers can occur locally that cannot be reflected by this relatively small spatially and temporally averaged $Wi$, which in fact is only a lower bound due to the polydispersity of the polymers (Crawford *et al.* 2008). Additionally, we conducted experiments with a different kind of polymer, polyethylene oxide (PEO, $Mw = 4 \times 10^6$ amu; Sigma Aldrich 189464), with $c$ varying from 0 to 210 ppm. Because of the relatively small $Wi$ for PEO (0.02 in this case), the effects are not as pronounced as those with PAM and the results with PEO will only be discussed in the heat transport measurement.

As the fluid viscosity changed significantly when polymers were added, the Rayleigh number for each polymer concentration was calculated using the measured

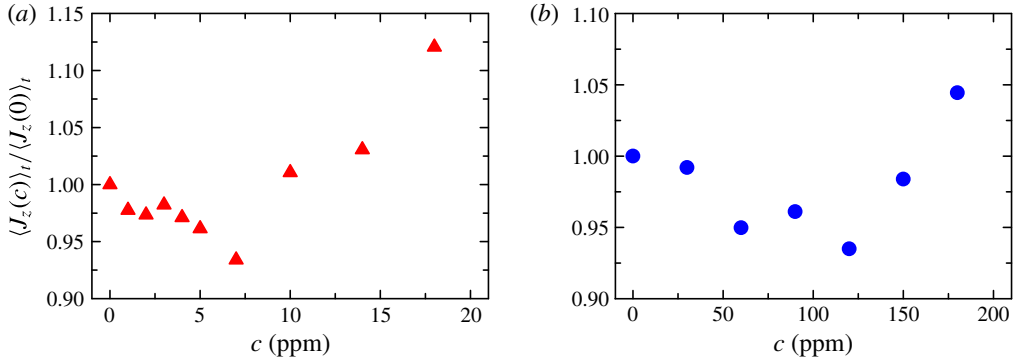


FIGURE 1. Time-averaged vertical heat flux $\langle J_z(c)\rangle_t$ as a function of polymer concentration $c$, normalized by its Newtonian value $\langle J_z(0)\rangle_t$ measured at the same $Ra$, for ($a$) PAM and ($b$) PEO.

viscosity and temperature difference $\Delta T$. As a result, the value of $Ra$ for PAM varied from $6.18 \times 10^9$ to $7.43 \times 10^9$ for $c$ between 0 and 24 ppm, and for PEO it varied from $6.22 \times 10^9$ to $5.44 \times 10^9$ for $c$ between 0 and 210 ppm. (It should be noted that for both types of polymer, the viscosity $\nu$ and temperature difference $\Delta T$ across the plates both increase with increase of $c$. In the case of PAM, the increase in $\Delta T$ more than compensates the increase in $\nu$ to result in an increase in $Ra$, whereas in the case of PEO, the combined results lead to a reduced $Ra$.) In order to compare the measured heat transfers with those in the absence of polymers, the local heat flux $\langle J_z(0)\rangle_t$ was measured as a function of $Ra$ without polymers and was used to normalize the measured heat flux $\langle J_z(c)\rangle_t$ at the same value of $Ra$. Here, $\langle\cdots\rangle_t$ denotes time average.

## 3. Results and discussion

We first show in figure 1 the time-averaged normalized vertical heat flux $\langle J_z(c)\rangle_t/\langle J_z(0)\rangle_t$ as a function of the polymer concentration $c$ for PAM and PEO. It is seen that, with polymer additives, the local heat flux first decreases a little and then starts to increase above a certain polymer concentration. The maximum enhancement of the local $Nu$ is $\sim$12 % for PAM at $c = 18$ ppm and $\sim$5 % for PEO at $c = 180$ ppm. These observed local $Nu$ dependences on $c$ are qualitatively similar to the global heat transport measurement made in the same cell with PEO (Wei *et al.* 2012). We note that if $c$ is further increased, i.e. beyond 18 ppm for PAM and 180 ppm for PEO, the heat transport drops.

To shed light on the mechanism of heat transport enhancement, we examine the probability density functions (PDFs) of the vertical heat flux $J_z$ and the horizontal heat flux $J_x$. The PDFs of $J_z$ at $c = 0$ and 18 ppm are plotted in figure 2($a$). We first look at the Newtonian case. It is seen that the PDF is skewed towards positive values. The negative tail of the PDF arises from the random velocity and temperature fluctuations and is referred to as incoherent heat flux hereafter. The positive tail, on the other hand, contains contributions from both incoherent fluxes and coherent fluxes that arise from the positively correlated velocity and temperature signals. The difference between the positive and negative tails gives rise to the net heat transport (Shang *et al.* 2003, 2004). The figure shows that, with polymer additives, the negative tail is strongly suppressed

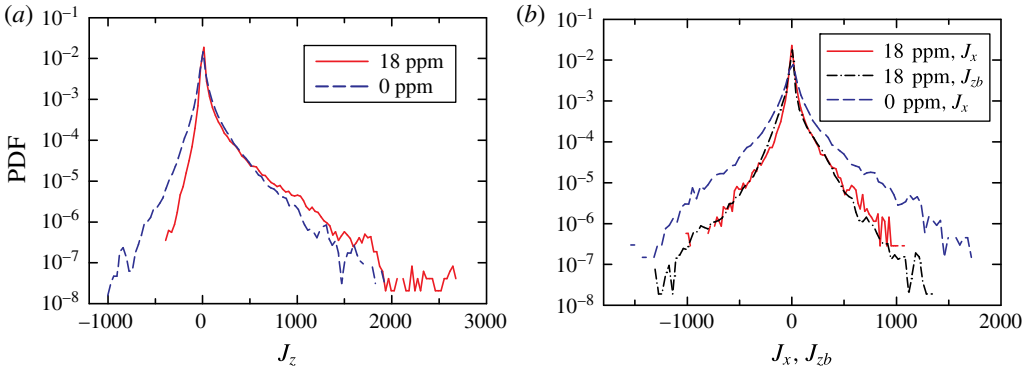


FIGURE 2. (*a*) Probability density functions of the vertical heat flux $J_z$ at $c = 0$ and $c =$ 18 ppm; (*b*) PDFs of the horizontal heat flux $J_x$ at $c = 0$ and $c = 18$ ppm. The black dashed-dot line is the vertical background heat flux $J_{zb}$ at $c = 18$ ppm. See the text for the definition of $J_{zb}$.

on one hand and very large values ($\geqslant$500) of instantaneous positive flux become more probable on the other hand. Thus, figure 2(*a*) suggests that the effects of polymer additives are to suppress the incoherent heat transport, and to enhance the coherent heat transport at the same time.

To confirm the above physical picture, we use a method introduced by Ching *et al.* (2004) to decompose $J_z$ into the heat flux carried by buoyant structures (i.e. plumes) and that by the turbulent background fluctuations, which is defined as

$$J_{zb}(t) = (u_{zb}(t) \times \delta T(t))H/(\kappa \Delta T), \tag{3.1}$$

where $u_{zb}(t) = u_z(t) - \langle u_z \mid T(t)\rangle$ is the velocity related to the random background fluctuations. It has been found in the Newtonian case that $J_{zb}$ and $J_x$ collapse almost perfectly on top of each other, indicating that the incoherent fluxes arising from turbulent background fluctuations are isotropic (Ching *et al.* 2004). A good collapse of $J_{zb}$ and $J_x$ is also observed in the present study for the case without polymers (not shown).

Figure 2(*b*) shows the PDFs of $J_{zb}$ and $J_x$ measured at $c = 18$ ppm, together with $J_x$ at $c = 0$ ppm. It is first seen that, consistent with the behaviour of the negative tail of the vertical heat flux shown in figure 2(*a*), in the presence of polymers the horizontal heat transport arising from the random background fluctuations, e.g. the incoherent heat flux, is highly suppressed compared with that of the Newtonian case. In addition, the incoherent parts of the vertical flux and the horizontal flux for the same polymer concentration essentially fall on top of each other, implying that in the presence of polymer additives the heat flux arising from turbulent background fluctuations in the bulk of the cell remains isotropic, as in the Newtonian case.

As thermal plumes are the primary heat carriers in turbulent thermal convection (Shang *et al.* 2003), the increase in the coherent part of the vertical flux suggests that the polymer additives may have altered the properties of the thermal plumes. To quantify this, we adopted a conditional averaging method similar to the one used by Huang *et al.* (2013) to identify the hot (cold) plumes based on the physical intuition that the temperature of a hot (cold) plume must be higher (lower) than that of the surrounding fluid. Operationally, we define a thermal plume as a time period when

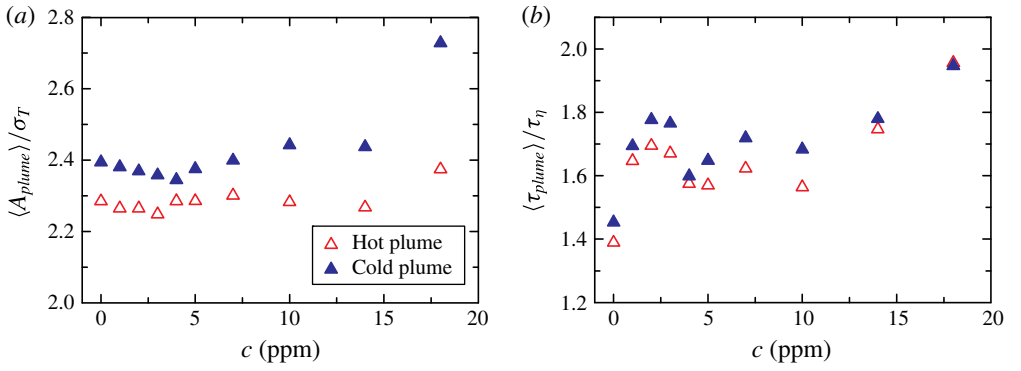


FIGURE 3. The average normalized plume amplitude $\langle A_{plume}\rangle/\sigma_T$ ($a$) and plume width $\langle \tau_{plume}\rangle/\tau_\eta$ ($b$) as a function of the polymer concentration $c$, where $\sigma_T$ and $\tau_\eta$ are respectively the r.m.s. temperature fluctuation and the Kolmogorov time scale.

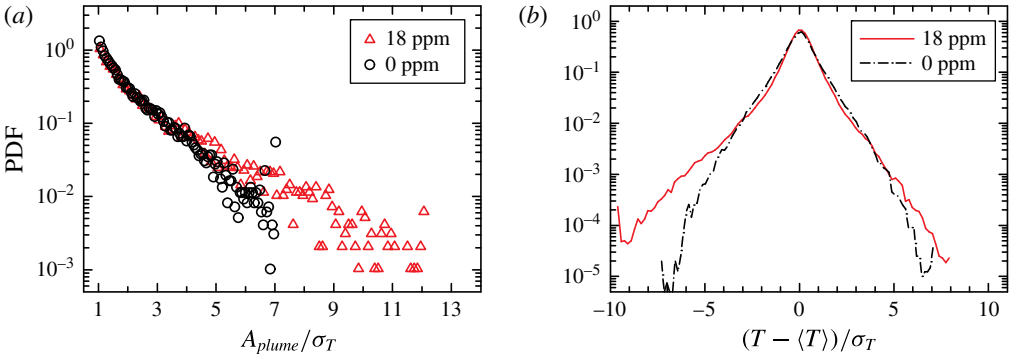


FIGURE 4. Probability density functions of ($a$) the normalized plume amplitude $A_{plume}/\sigma_T$ and ($b$) the normalized temperature fluctuation $(T-\langle T\rangle)/\sigma_T$.

$\pm[T(t)-\langle T\rangle_t] > b\sigma_T$, with $b = 1.5$ being a threshold parameter, $\sigma_T = \sqrt{\langle (T-\langle T\rangle)^2\rangle}$ being the root-mean-square (r.m.s.) temperature fluctuation, '+' for hot plumes and '−' for cold plumes. The width of a plume $\tau_{plume}$ is defined as the length of the consecutive time segment that satisfies the above criterion in the measured temperature time series. The amplitude of a plume $A_{plume}$ is then defined as the absolute value of the largest temperature deviation from the mean within this time segment. We tried different values of $b$ from 0.8 to 3 and the statistical properties based on different values of $b$ remained unchanged.

In figure 3($a$) we plot the normalized average plume amplitude $\langle A_{plume}\rangle/\sigma_T$ as a function of $c$. It is seen that the dependence of the plume amplitude $A_{plume}$ on $c$ has a qualitatively similar trend to that of the local $Nu$, i.e. the plume amplitude first drops a little when polymers are added and then increases when $c$ is beyond a certain value. A similar trend was observed for the average normalized plume width $\langle \tau_{plume}\rangle/\tau_\eta$, as shown in figure 3($b$), i.e. with increase of $c$, $\tau_{plume}$ increases. The PDFs of $A_{plume}/\sigma_T$ for $c = 0$ and 18 ppm are shown in figure 4($a$). It is seen that with polymer additives plumes with larger amplitudes become more probable compared with the Newtonian case. The increased $A_{plume}$ implies that large temperature deviations from the mean would be more probable with polymer additives, which is confirmed by the higher

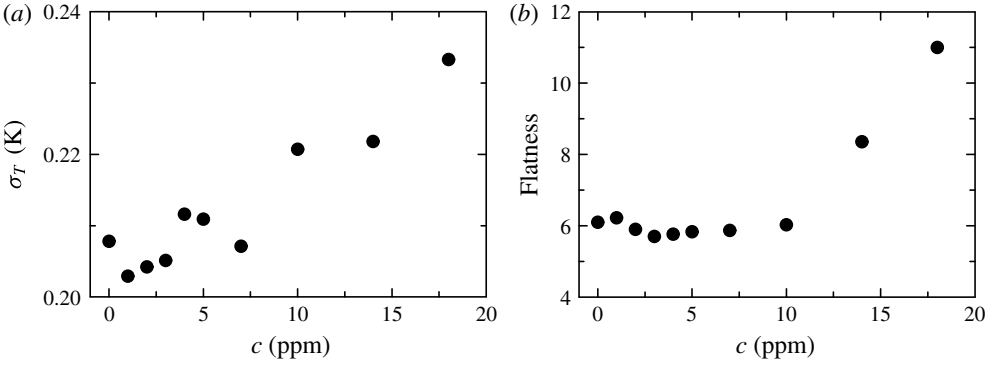


FIGURE 5. The temperature r.m.s. $\sigma_T$ (*a*) and flatness (*b*) as a function of the polymer concentration $c$.

tails of the PDF of the normalized temperature fluctuations for $c = 18$ ppm compared with the Newtonian case, as shown in figure 4(*b*). Both larger $A_{plume}$ and $\tau_{plume}$ imply that thermal plumes have become more coherent with polymer additives. A feature we have noticed is that the increased temperature deviation from the mean or the increase in plume amplitude only becomes significant when $c$ is sufficiently high. For example, at $c = 7$ ppm the temperature PDF is essentially the same as in the $c = 0$ case (not shown).

One may also notice from figure 4(*b*) that the PDF at $c = 18$ ppm is asymmetric, indicating that the cold plumes undergo more significant changes than the hot ones. This different behaviour is also revealed in $A_{plume}$ and $\tau_{plume}$ (see figure 3). Recently, Traore, Castelain & Burghelea (2015) have shown that the $\tau_p$ of PAM has a very strong negative dependence on temperature. For example, they have found that the $\tau_p$ of PAM can increase by two orders of magnitude when the temperature is decreased from ∼35 to ∼5 °C. Therefore, polymers in a parcel of hot fluid will interact with the turbulent flow differently from those in a parcel of cold fluid. This also supports the idea of a local *Wi* that can be much larger than the one based on globally averaged properties.

We also found that the local temperature fluctuation $\sigma_T$ increases with $c$, as shown in figure 5(*a*), and has a similar $c$ dependence to $J_z$. A similar observation was reported in a direct numerical simulation study of homogeneous RBC with polymer additives (Benzi *et al.* 2010). Moreover, the temperature flatness, which is defined as $\langle (T - \langle T \rangle)^4 \rangle / \sigma_T^4$, shown in figure 5(*b*), increases from 6 at $c = 0$ ppm to 11 at $c = 18$ ppm, also suggesting that the rare but large deviations from the mean are more probable with polymer additives.

In addition to the temperature field, the velocity field also becomes more coherent with polymer additives, which is quantified by the autocorrelation functions of the vertical velocity $u_z$ and the horizontal velocity $u_x$ measured at different values of $c$. It is seen from figure 6(*a*) that with increasing $c$, the decay of the autocorrelation functions for $u_z$ becomes slower, suggesting an enhancement of the coherency of the velocity field. The enhanced coherence in $u_x$ is manifested by the increased number of oscillation periods in the autocorrelation function shown in figure 6(*b*). Figure 6(*c*) shows that the degree of correlation between the velocity and the temperature increases with increasing polymer concentration, which is further evidence that the coherence of thermal plumes is increased by polymer additives, as the velocity and

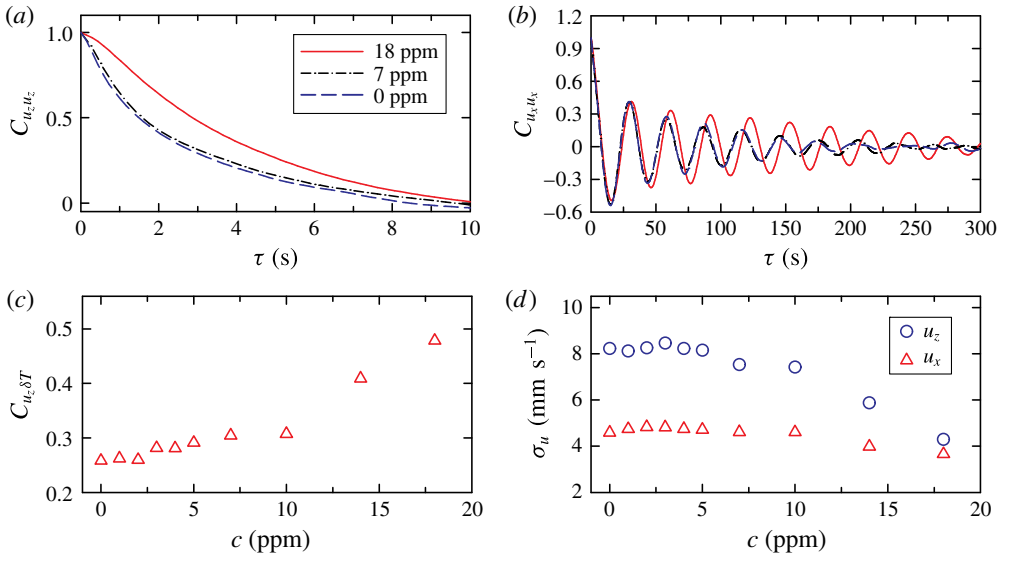


FIGURE 6. Autocorrelation functions of the vertical velocity $u_z$ (*a*) and the horizontal velocity $u_x$ (*b*) at polymer concentrations of $c = 0$, 7 and 18 ppm. (*c*) Correlation coefficient between the temperature deviation $\delta T$ from the mean and the vertical velocity $u_z$ as a function of $c$. (*d*) The r.m.s. velocity $\sigma_u$ as a function of $c$ for the vertical and horizontal velocities.

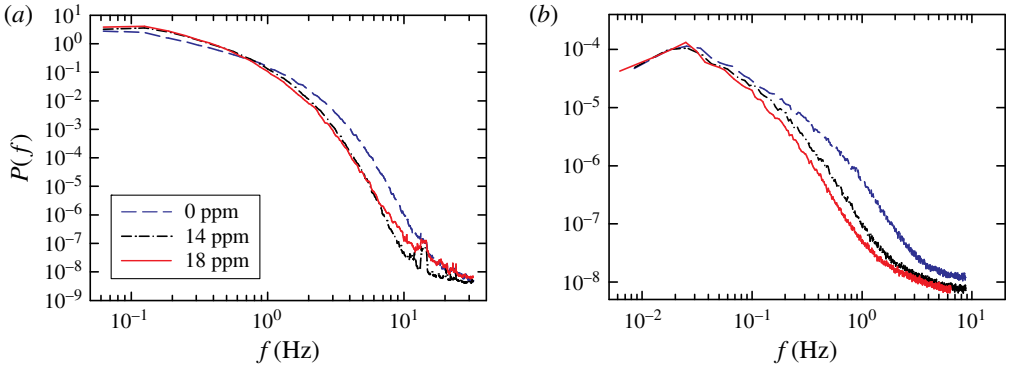


FIGURE 7. (*a*) Power spectra of the temperature at $c = 0$, 14 and 18 ppm. (*b*) The corresponding power spectra of the velocity.

temperature of thermal plumes should be correlated. Again, we note from the above that the increase of plume coherency only becomes significant when $c$ is above a certain threshold value. At lower $c$, these properties remain essentially the same as in the Newtonian case. In figure 6(*d*) we show the r.m.s. velocity $\sigma_u$ as a function of $c$. It is seen that $\sigma_u$ decreases with increasing $c$, suggesting that the velocity fluctuations are suppressed by polymers.

To gain further insight into the possible mechanism that leads to the enhancement of plume coherency, we examine the power spectra of both the temperature and the velocity fluctuations for several polymer concentrations, as shown in figure 7.

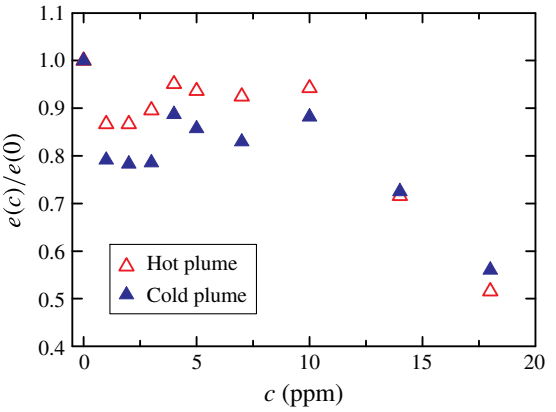


FIGURE 8. The plume emission rate $e(c)$ normalized by the Newtonian value $e(0)$ as a function of the polymer concentration $c$.

The magnitudes of both the temperature and the velocity spectra at high frequencies are seen to decrease significantly with increasing $c$, which implies that polymers suppress turbulent fluctuations at small scales. Similar observations were reported in a direct numerical simulation study of Rayleigh–Taylor turbulence (Boffetta *et al.* 2010). It should be noted that there is a cross-over for the temperature power spectra for cases with and without polymer at $f_c \simeq 0.7$ Hz. For frequencies smaller than $f_c$ (corresponding to larger length scales), the energy contained in these scales is larger than the Newtonian case, and it is smaller for frequencies larger than $f_c$, suggesting that there is a redistribution of thermal energy among different scales when polymers are added to the flow. For the velocity power spectra, a suppression of turbulent kinetic energy at small scales is also observed. However, the situation is somewhat different, in the sense that a cross-over to energy at the large scale is not observed. It is seen that the turbulent kinetic energy decreases at all scales smaller than the energy injection scale when polymers are added, and the degree of energy quenching increases with increase of $c$. The different behaviours of the temperature and velocity power spectra at small frequencies (large scales) are consistent with the observation in Benzi *et al.* (2010), where it was found that polymers strongly modify the large scale of the temperature field, while having negligible effects on the large scale of the velocity field. There has been evidence that the energy of turbulent fluctuations in turbulent RBC is supplied by thermal plumes (Xia, Sun & Zhou 2003). When polymers are added to the flow, the small-scale turbulent fluctuations are suppressed, as suggested by the reduction of the velocity fluctuation $\sigma_u$ shown in figure 6(*d*) and the power spectra of the velocity fluctuations in figure 7(*b*). Thermal plumes thus supply less energy to the turbulence, and they are more energetic and able to transport heat more efficiently.

We note that as the plume emissions are manifestations of thermal BL instability in turbulent RBC (Malkus 1954), the effects of polymer additives on BLs may be examined indirectly by estimating the plume emission rate $e$. Using the aforementioned extracted plumes we obtain the plume emission rate $e$ in units of plume number per hour. The dependence on $c$ of $e(c)$ normalized by its Newtonian value $e(0)$ is shown in figure 8. It is clearly seen that with increase of $c$, $e$ decreases. Remarkably, $e$ is very sensitive to polymer additives, e.g. upon the addition of 1 ppm of polymers,

$e$ drops by $\sim$15 % compared with the Newtonian case. These observations provide evidence for the proposed stabilization of the thermal BL and the resulting reduction of plume emissions by polymer additives (Ahlers & Nikolaenko 2010; Wei *et al.* 2012).

Finally, we remark that there appears to exist a certain polymer concentration, only beyond which significant heat transport enhancement can be achieved. The existence of such a threshold concentration may be seen from a number of figures, such as figure 1, where it is seen to be around 7 ppm for PAM and around 120 ppm for PEO. This threshold $c$, though not very sharp, may be understood in such a way that the enhancement of plume coherency requires more polymers than the stabilization of the boundary layer, which is supported by the $c$ dependence of $A_{plume}$ and $\tau_{plume}$ (figure 3) as well as the temperature r.m.s. $\sigma_T$ (figure 5) and the autocorrelation function of the velocity $u_\alpha$ (figure 6*a*,*b*), all of which undergo significant changes only when $c$ is beyond a certain value. Therefore, the local heat flux first decreases gradually due to the reduction of plume emissions before the significant enhancement starts.

## 4. Concluding remarks

In summary, we have demonstrated that polymer additives can significantly enhance heat transport in the bulk of turbulent thermal convection. The enhancement occurs concurrently with the increased coherency of thermal plumes. It is found that the effects of polymer additives in the bulk of turbulent thermal convection are to suppress the random turbulent fluctuations on one hand, and to increase the coherence of the temperature and velocity fields on the other hand, i.e. they suppress the incoherent heat transfer and enhance the coherent heat transfer. The effects of polymer additives on the BL are indirectly examined by studying the plume emission rate $e$. The reduction of $e$ with increase of $c$ indicates a stabilization of the thermal BL by polymer additives. This can be achieved through two routes. One is through the reduced bulk velocity fluctuations that constantly perturb the BL (Zhou & Xia 2010); the other is through the increased viscosity, which leads to a more stable viscous BL (Benzi *et al.* 2012). As the viscous and thermal BLs are strongly coupled (Zhou *et al.* 2010), this will result in a more stable thermal BL. In this context, the present experiment supports the idea that the combined effects of enhancement of plume coherency in the turbulent bulk flow and reduction of plume emission in the BL determine whether the global heat transport will be enhanced or reduced in turbulent thermal convection with polymer additives (Ahlers & Nikolaenko 2010; Benzi *et al.* 2010; Wei *et al.* 2012). Finally, we remark that the decrease of $J_z$ beyond $c = 18$ ppm for PAM and 180 ppm for PEO may be viewed as the result of the effect of reduced plume emission overtaking the effect of enhanced plume coherency.

## Acknowledgements

This work was supported in part by the Hong Kong Research Grant Council under grant numbers CUHK 403712 and 404513, and in part by a grant from the PROCORE-France/Hong Kong Joint Research Scheme sponsored by the Research Grants Council of Hong Kong and the Consulate General of France in Hong Kong (reference no. F-HK19/11T).

## References


AHLERS, G., GROSSMANN, S. & LOHSE, D. 2009 Heat transfer and large-scale dynamics in turbulent Rayleigh–Bénard convection. *Rev. Mod. Phys.* **81**, 503–537.

AHLERS, G. & NIKOLAENKO, A. 2010 Effect of a polymer additive on heat transport in turbulent Rayleigh–Bénard convection. *Phys. Rev. Lett.* **104**, 034503.

BENZI, R., CHING, E. S. C. & DE ANGELIS, E. 2010 Effect of polymer additives on heat transport in turbulent thermal convection. *Phys. Rev. Lett.* **104**, 024502.

BENZI, R., CHING, E. S. C. & CHU, V. W. S. 2012 Heat transport by laminar boundary layer flow with polymers. *J. Fluid Mech.* **696**, 330–344.

BOFFETTA, G., MAZZINO, A., MUSACCHIO, S. & VOZELLA, L. 2010 Polymer heat transport enhancement in thermal convection: the case of Rayleigh–Taylor turbulence. *Phys. Rev. Lett.* **104**, 184501.

CALZAVARINI, E., LOHSE, D., TOSCHI, F. & TRIPICCIONE, R. 2005 Rayleigh and Prandtl number scaling in the bulk of Rayleigh–Bénard turbulence. *Phys. Fluids* **17**, 055107.

CHILLÁ, F. & SCHUMACHER, J. 2012 New perspectives in turbulent Rayleigh–Bénard convection. *Eur. Phys. J.* E **35**, 58.

CHING, E. S. C., GUO, H., SHANG, X.-D., TONG, P. & XIA, K.-Q. 2004 Extraction of plumes in turbulent thermal convection. *Phys. Rev. Lett.* **93**, 124501.

CRAWFORD, A. M., MORDANT, N., XU, H. & BODENSCHATZ, E. 2008 Fluid acceleration in the bulk of turbulent dilute polymer solutions. *New J. Phys.* **10**, 123015.

HUANG, S.-D., KACZOROWSKI, M., NI, R. & XIA, K.-Q. 2013 Confinement-induced heat-transport enhancement in turbulent thermal convection. *Phys. Rev. Lett.* **111**, 104501.

LOHSE, D. & TOSCHI, F. 2003 Ultimate state of thermal convection. *Phys. Rev. Lett.* **90**, 034502.

LOHSE, D. & XIA, K.-Q. 2010 Small-scale properties of turbulent Rayleigh–Bénard convection. *Annu. Rev. Fluid Mech.* **42**, 335–364.

MALKUS, W. V. R. 1954 The heat transport and spectrum of thermal turbulence. *Proc. R. Soc. Lond.* A **225**, 196–212.

OUELLETTE, N. T., XU, H. & BODENSCHATZ, E. 2009 Bulk turbulence in dilute polymer solutions. *J. Fluid Mech.* **629**, 375–385.

PROCACCIA, I., L'VOV, V. S. & BENZI, R. 2008 Theory of drag reduction by polymers in wall-bounded turbulence. *Rev. Mod. Phys.* **80**, 225–247.

QIU, X.-L., XIA, K.-Q. & TONG, P. 2005 Experimental study of velocity boundary layer near a rough conducting surface in turbulent natural convection. *J. Turbul.* **6**, N30.

RUBINSTEIN, M. & COLBY, R. H. 2003 *Polymer Physics*. Oxford University Press.

SHANG, X.-D., QIU, X.-L., TONG, P. & XIA, K.-Q. 2003 Measured local heat transport in turbulent Rayleigh–Bénard convection. *Phys. Rev. Lett.* **90**, 074501.

SHANG, X.-D., QIU, X.-L., TONG, P. & XIA, K.-Q. 2004 Measurements of the local convective heat flux in turbulent Rayleigh–Bénard convection. *Phys. Rev.* E **70**, 026308.

SUN, C., CHEUNG, Y.-H. & XIA, K.-Q. 2008 Experimental studies of the viscous boundary layer properties in turbulent Rayleigh–Bénard convection. *J. Fluid Mech.* **605**, 79–113.

TOMS, B. A. 1948 Some observations on the flow of linear polymer solutions through straight tubes at large Reynolds numbers. In *Proceedings of the First International Rheological Congress*, vol. 2, pp. 135–141.

TRAORE, B., CASTELAIN, C. & BURGHELEA, T. 2015 Efficient heat transfer in a regime of elastic turbulence. *J. Non-Newtonian Fluid Mech.* **223**, 62–76.

WEI, P., CHAN, T.-S., NI, R., ZHAO, X.-Z. & XIA, K.-Q. 2014 Heat transport properties of plates with smooth and rough surfaces in turbulent thermal convection. *J. Fluid Mech.* **740**, 28–46.

WEI, P., NI, R. & XIA, K.-Q. 2012 Enhanced and reduced heat transport in turbulent thermal convection with polymer additives. *Phys. Rev.* E **86**, 016325.

XI, H.-D., BODENSCHATZ, E. & XU, H. 2013 Elastic energy flux by flexible polymers in fluid turbulence. *Phys. Rev. Lett.* **111**, 024501.

XIA, K.-Q. 2013 Current trends and future directions in turbulent thermal convection. *Theor. Appl. Mech. Lett.* **3**, 052001.

XIA, K.-Q., SUN, C. & ZHOU, S.-Q. 2003 Particle image velocimetry measurement of the velocity field in turbulent thermal convection. *Phys. Rev.* E **68**, 066303.

ZHOU, Q., STEVENS, R. J. A. M., SUGIYAMA, K., GROSSMANN, S., LOHSE, D. & XIA, K.-Q. 2010 Prandtl–Blasius temperature and velocity boundary-layer profiles in turbulent Rayleigh–Bénard convection. *J. Fluid Mech.* **664**, 297–312.

ZHOU, Q. & XIA, K.-Q. 2010 Measured instantaneous viscous boundary layer in turbulent Rayleigh–Bénard convection. *Phys. Rev. Lett.* **104**, 104301.

ZIMM, B. H. 1956 Dynamics of polymer molecules in dilute solution: viscoelasticity, flow birefringence and dielectric loss. *J. Chem. Phys.* **24**, 269–278.